Am J Physiol Cell Physiol
279: C1495–C1505, 2000.

Calcium regulates estrogen increase in permeability of cultured CaSki epithelium by eNOS-dependent mechanism

GEORGE I. GORODESKI
Departments of Reproductive Biology and Physiology and Biophysics, Case Western Reserve University School of Medicine, Cleveland, Ohio 44106

Received 24 January 2000; accepted in final form 5 June 2000

Gorodeski, George I. Calcium regulates estrogen increase in permeability of cultured CaSki epithelium by eNOS-dependent mechanism. *Am J Physiol Cell Physiol* 279: C1495–C1505, 2000.—Estrogen increases baseline transepithelial permeability across CaSki cultures and augments the increase in permeability in response to hypertonic gradients. In estrogen-treated cells, lowering cytosolic calcium abrogated the hypertonicity-induced augmented increase in permeability and decreased baseline permeability to a greater degree than in estrogen-deprived cells. Steady-state levels of cytosolic calcium in estrogen-deprived cells were higher than in estrogen-treated cells. Increases in extracellular calcium increased cytosolic calcium more in estrogen-deprived cells than in estrogen-treated cells. However, in estrogen-treated cells, increasing cytosolic calcium was associated with greater increases in permeability in response to hypertonic gradients than in estrogen-deprived cells. Lowering cytosolic calcium blocked the estrogen-induced increase in nitric oxide (NO) release and in the in vitro conversion of L-[^{3}H]arginine to L-[^{3}H]citrulline. Treatment with estrogen upregulated mRNA of the NO synthase isoform endothelial nitric oxide synthase (eNOS). These results indicate that cytosolic calcium mediates the responses to estrogen and suggest that the estrogen increase in permeability and the augmented increase in permeability in response to hypertonicity involve an increase in NO synthesis by upregulation of the calcium-dependent eNOS.

paracellular permeability; transepithelial transport; cervical mucus; cytosolic calcium; nitric oxide; nitric oxide synthase; G-actin; cytoskeleton; endothelial nitric oxide synthase

THE MAIN FUNCTION OF THE UTERINE cervical epithelium is to control secretion of cervical mucus. The cervical mucus is important for reproduction and for woman's health. Abnormal secretion of cervical mucus may lead to infertility and to states of disease such as mucorrhea and dryness dyspareunia (14).

The cervical mucus is a mixture of mucins and cervical plasma. Mucins are secreted in the cervical canal by exocytosis from endocervical cells (14). The cervical plasma composes 80–99% of the total weight of the cervical mucus, and it originates by transudation of fluid from the blood (14). The driving force is the blood pressure: it generates a hydrostatic gradient between the capillaries and the cervical canal and compels movement of fluid through the intercellular (paracellular) space into the lumen (48). Cervical epithelial cells control the free movement of fluid through the cervix by forming two functional barriers: the tight junctional resistance (R_{TJ}) and the resistance of the lateral intercellular space (R_{LIS}; see Ref. 15). According to the equivalent electrical circuit model of ion transport the sum of R_{TJ} and R_{LIS} in series determines the overall permeability of the cervical epithelium (41, 47).

In human cervical epithelial cells, the R_{TJ} and R_{LIS} can be independently regulated (15), but the mechanisms of regulation are not entirely understood. An example is the effect of estrogen on cervical permeability. Estrogen increases cervical secretions in women (14). Studies at the cellular level revealed that the effect of estrogen involves an increase in R_{LIS} (16) and is mediated by estrogen receptor α-activation of the nitric oxide (NO)/cGMP-dependent increase in G-actin (18, 24). The proposed molecular mechanism of increase in permeability is modulation of the cytoskeleton. By shifting actin steady state toward G-actin, estrogen stimulates transformation of the cytoskeleton in a more flexible structure (16). This renders cervical epithelial cells more deformable in response to the prevailing blood pressure-induced hydrostatic pressure and results in a greater decrease in R_{LIS} and an increase in the permeability (16, 17).

Calcium regulates paracellular permeability of cultured human cervical epithelia (23). Calcium increases the R_{TJ} by maintaining the tight junctional elements in a closed state (27). Also, fluctuations in cytosolic calcium can modulate agonist-induced changes in R_{TJ} and the R_{LIS} (23, 25, 27). Until recently, little was known about the role of calcium in the responses to estrogen. Calcium levels in cervical secretions change during the cycle (14), suggesting that estrogen modulates transcervical transport of calcium. Changes in extracellular calcium can regulate paracellular permeability directly by changing the gating status of the tight junctions (27) or indirectly by modulating levels of cytosolic calcium (23). Consequently, if estrogen signaling depends on calcium signaling, changes in extracel-

Address for reprint requests and other correspondence: G. I. Gorodeski, Univ. MacDonald Women's Hospital, Univ. Hospitals of Cleveland, 11100 Euclid Ave., Cleveland, OH 44106 (E-mail: gig@po.cwru.edu).

The costs of publication of this article were defrayed in part by the payment of page charges. The article must therefore be hereby marked "*advertisement*" in accordance with 18 U.S.C. Section 1734 solely to indicate this fact.

lular calcium can affect the estrogen increase in cervical secretions by modulation of intracellular calcium activity. The objective of the present study was to determine the degree to which changes in cytosolic calcium modulate the effect of estrogen on cervical permeability.

METHODS

Cell cultures. The experiments utilized CaSki cells, which are a stable line of transformed cervical epithelial cells that express phenotypic markers of the endocervix (26). Cells were grown and maintained in a culture dish at 37°C in a 91% O_2-9% CO_2 humidified incubator and were routinely tested for mycoplasma. For experiments, cells were plated on filters for 8 h and then shifted to steroid-free medium (16). After 3 days, cells were treated with 10 nM 17β-estradiol (estrogen-treated cells) or the vehicle (estrogen-deprived cells) for two additional days. Before assays, filters containing cells were washed three times and preincubated for 15 min at 37°C in a modified Ringer buffer (16, 24).

Changes in paracellular permeability. Changes in paracellular permeability were determined in terms of changes in transepithelial electrical conductance (G_{TE}). Changes in G_{TE} were determined continuously across filters mounted vertically in a modified Ussing chamber from successive measurements of transepithelial electrical current (ΔI) and of the transepithelial potential difference (ΔPD, lumen negative): $G_{TE} = \Delta I/\Delta PD$. Transepithelial hypertonic gradients in the subluminal to luminal direction were established by adding aliquots of 2 M sucrose solution to the subluminal solution (15, 20).

Determinations of cytosolic calcium. Determinations of cytosolic calcium in cells attached on filters were published previously (28). Briefly, cells on filters were loaded with 7 μM fura 2, and measurements of fluorescence were conducted in a custom-designed fluorescence chamber as described (4, 28). Cells were illuminated over the apical surface, and the intensity of the emitted light from the apical surface was measured. Changes in cytosolic calcium were determined by switching the excitation filters to record the maximal (340-nm excitation/510-nm emission) and minimal (380-nm excitation/510-nm emission) fluorescence for cytosolic calcium determinations (4, 28) and were calculated according to the formula $[Ca^{2+}]_i$ (nM) = $[(R - R_{min})/(R_{max} - R)] \cdot K_d \cdot (S_{f2}/S_{b2})$ (30), where $[Ca^{2+}]_i$ is the level of cytosolic calcium, R is the ratio of fluorescence excitation measurements at 340 to 380 nm, R_{min} and R_{max} are the experimentally determined minimum and maximum calcium measurement ratios at 340 and 380 nm, respectively, K_d is the dissociation constant for fura 2 (224 nM), and S_{f2}/S_{b2} is the ratio of fluorescence value at 380-nm excitation determined at R_{min} (0 calcium) and R_{max} (maximal calcium). Maximal calcium fluorescence was obtained by adding 10 μM ionomycin in the presence of 10 mM $CaCl_2$, and minimal calcium fluorescence was obtained by competing calcium from fura 2 with 2.5 mM $MnCl_2$.

Determinations of free calcium. Levels of calcium in the extracellular buffer were manipulated using the calcium chelator EGTA. Concentrations of free calcium in the extracellular buffer were calculated as described (23, 25).

DNase I inhibition assay. DNase I inhibition assay was described (16). G-actin content in lysates of cells grown on filters was determined in terms of DNase I inhibition of DNA degradation, based on the fact that under the conditions of the experiment the main inhibitor of DNase I is G-actin (2). Total actin was measured by incubating lysates with guanidine hydrochloride to depolymerize F-actin to monomeric G-actin. Data of the G-actin and total cellular actin were expressed per milligram total protein.

Release of NO. Release of NO was determined as the accumulation of nitrite and nitrate in the extracellular medium by a modified Greiss method as described (4). The detection limit of the assay was 2 μM, and results were expressed as picomoles per minute per milligram of protein.

Nitric oxide synthase activity. Nitric oxide synthase (NOS) activity was assayed by following the conversion of L-[2,3,4,5-^{3}H]arginine to L-[2,3,4,5-^{3}H]citrulline as described (43) with modifications. Before experiments, cells on filters were washed three times with PBS (37°C) and lysed on ice for 20 s with buffer (1 μl/10^4 cells at 20°C, pH 7.4) containing 320 mM sucrose, 0.1 mM EDTA, 1 mM dithiothreitol, 10 mM HEPES, 10 μg/ml soybean trypsin inhibitor, 10 μg/ml leupeptin, and 2 μg/ml aprotinin. Aliquots were removed for DNA. The lysates were centrifuged (10^4 *g* for 20 min at 4°C), and the supernatants were assayed in triplicate. The supernatant (100 μl, about 200 μg of cell protein) was incubated with 100 μl of buffer (40 mM potassium phosphate, pH 7.4, 8 mM L-valine, 100 μM NADPH, 1 mM $MgCl_2$, 1 mM $CaCl_2$, 100 μM L-arginine, 25 μM FAD, 25 μM FMN, 5 μM tetrahydrobiopterin, 100 μM phenylmethylsulfonyl fluoride, and 0.2 μM calmodulin) plus L-[2,3,4,5-^{3}H]arginine monohydrochloride. Assays were also carried out in the presence of 1.2 mM EGTA, 1 mM N^G-nitro-L-arginine methyl ester (L-NAME), 1 mM N^G-nitro-L-arginine (L-NA), or 1 mM N^G-monomethyl-L-arginine (L-NMMA). Samples were incubated for 30 min at 37°C before the reaction was terminated by adding 500 μl of H_2O-Dowex-50W (1:1 vol/vol; Na^+ form). The resin-incubated mixture was dispersed and diluted by adding 860 μl of 2dH_2O. The resin was allowed to settle for 15 min, and 975 μl of supernatant were pipetted into scintillation vials. Scintillation counting fluid (10 ml) was added to each vial, and the radioactivity corresponding to L-[2,3,4,5-^{3}H]citrulline was measured. NOS activity was expressed as picomoles per minute per milligram of DNA. The calcium-dependent NOS activity was determined from the difference between activities obtained in control and in EGTA (or L-NAME, L-NA, or L-NMMA) buffers; total activity of the NOS was determined by subtracting the activities obtained in EGTA plus L-NAME buffers.

Molecular biology methods. Molecular biology methods were described (19). Total RNA from cultured cells was isolated with the Qiagen kit (Qiagen, Chatsworth, CA; see Ref. 19). The method for RT-PCR was described (19). The following PCR conditions were applied: for endothelial nitric oxide synthase (eNOS), 35 cycles of 1-min denaturation step at 94°C, 1 min of annealing step at 62°C, and 2 min of extension step at 72°C; for neuronal (brain) nitric oxide synthase (bNOS), 35 cycles of 1 min at 94°C, 2 min at 56°C, and 2 min at 72°C; for the inducible nitric oxide synthase (iNOS), 35 cycles of 1 min at 94°C, 2 min at 56°C, and 2 min at 72°C. The following oligonucleotide primers were used: human eNOS (34) 5′-forward (sense) 5′-CAG TGT CCA ACA TGC TGC TGG AAA TTG-3′, 3′-reverse (antisense) 5′-TAA AGG TCT TCT TGG TGA TGC C-3′; human bNOS (38) 5′-forward (sense) 5′-TTT CCG AAG CTT CTG GCA ACA GCG GCA ATT-3′, 3′-reverse (antisense) 5′-GGA CTC AGA TCT AAG GCG GTT GGT CAC TTC-3′; iNOS (11) 5′-forward (sense) 5′-GCC TCG CTC TGG AAA GA-3′, 3′-reverse (antisense) 5′-TCC ATG CAG ACA ACC TT-3′. X-ray films were analyzed with a laser densitometer Sciscan 5000 (United States Biochemical, Cleveland, OH) and normalized relative to glyceraldehyde-3-phosphate dehydrogenase (GAPDH) RNA (19).

Total protein and total DNA. Total protein and total DNA were measured as described (21, 22).

Cell viability. Cell viability was determined by mitochondrial respiration assay using dimethylthiazol diphenyl tetrazolium (MTT) staining (46). Cells on filters were incubated for 60 min at 37°C in Ringer buffer containing 1 mg/ml MTT. Cultures were washed with PBS and solubilized in isopropanol containing 0.1 M HCl and 1% Triton X-100. Lysates were mixed by pipetting to dissolve the reduced MTT crystals and were spun at 10,000 *g* for 5 min. The solubilized formazan was measured by determining absorption at 575 nm minus background absorbance at 690 nm for each sample. In control experiments, cells were treated for 30 min with 50 μM of the protonophore uncoupler carbonyl cyanide *m*-chlorophenylhydrazone (mClCCP; Aldrich, Milwaukee, WI). Viability was defined as <5% positive staining compared with control (mClCCP-treated) cells.

Drugs treatments. For experiments with cells on filters, all reagents, except sucrose, were added from concentrated (1,000–300×) stocks (pH 7.2) of saline, PBS, ethanol, or DMSO to both the luminal and subluminal solutions. Aliquots of sucrose solution were added only to the subluminal solution.

Statistical analysis of the data. Data are presented as means ± SD, and significance of differences among means was estimated by ANOVA. Trends were calculated using GB-STAT V5.3 (Dynamic Microsystems, Silver Spring, MD) and were analyzed with ANOVA. Best fit of regression equations (least squares criterion) was achieved with SlideWrite Plus (Advanced Graphics Software, Carlsbad, CA), which uses the Levenberg-Marquardt Algorithm, and was analyzed using ANOVA.

Chemicals and supplies. L-[2,3,4,5-^{3}H]arginine monohydrochloride was obtained from American Radiolabled Chemicals (St. Louis, MO). Anocell (Anocell-10) filters were obtained from Anotec (Oxon, UK). Fluorescent microspheres (FluoresBrite beads, calibration grade) were obtained from Polysciences (Warrington, PA). All other chemicals were obtained from Sigma Chemicals.

RESULTS

Experimental design to test effects of cytosolic calcium on paracellular permeability. The main objective of the study was to determine the degree to which changes in cytosolic calcium affect the estrogen-induced increases in paracellular permeability. To manipulate cytosolic calcium, CaSki cells attached on filters were exposed to the following conditions.

To increase cytosolic calcium, extracellular calcium was increased above the physiological level of 1.2 mM to augment calcium influx. In cells grown in regular medium, raising extracellular calcium from 1.2 to 4.0 mM increased cytosolic calcium from 89 to 97 nM ($P < 0.01$, paired *t*-test), but it had no effect on G_{TE} (Fig. 1*A*).

To decrease cytosolic calcium, cells were treated with EGTA to lower extracellular calcium and to decrease calcium influx (23). In cells grown in regular medium, lowering extracellular calcium from 1.2 to 0.6 mM decreased cytosolic calcium acutely from 91 ± 5 to 66 ± 5 nM ($P < 0.01$, paired *t*-test; Fig. 2). Lowering extracellular calcium also increased G_{TE} acutely (Fig. 2). The effect of low extracellular calcium on G_{TE} could be the result of an effect on the tight junctions at extracellular sites [by changing the gating properties of the tight junctional elements (25, 27)] or secondary to lowered cytosolic calcium (13, 31). To discern between these two mechanisms, it was necessary to abrogate the low-calcium-related increase in G_{TE} that was induced by direct modulation of the tight junctions. This was done by adding $MnCl_2$ at equimolar concentrations to the calcium that was chelated by EGTA (27). As is shown in Fig. 2, $MnCl_2$ reversed the increase in G_{TE}; the mechanism of Mn^{2+} action on G_{TE} is unknown, but it is not the result of changes in cytosolic calcium, since

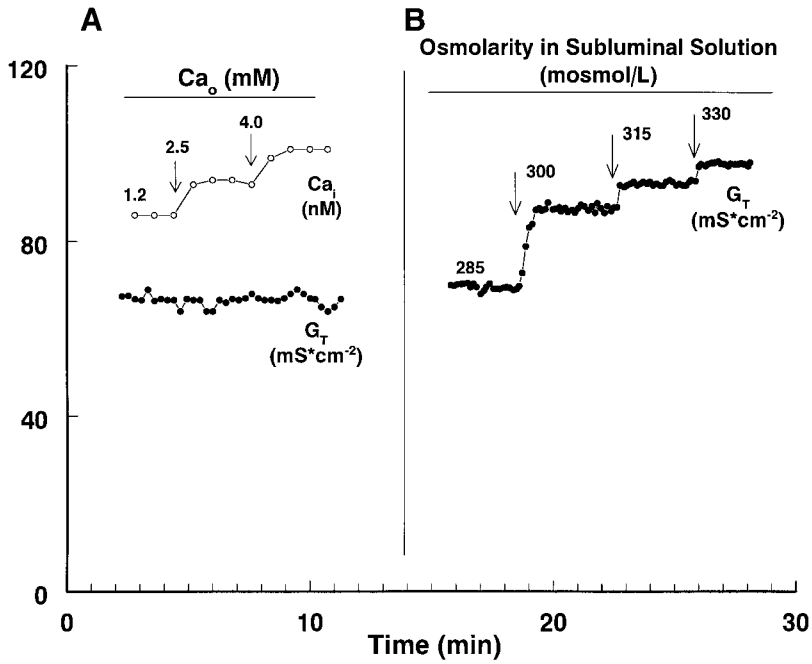

Fig. 1. *A*: effects of increasing extracellular calcium (Ca_o) on cytosolic calcium (Ca_i) and on transepithelial electrical conductance (G_{TE}).Shown is an experiment done on CaSki cells plated on filters and maintained in regular culture medium. Determinations of Ca_i levels were done in the fluorescence chamber (○, see METHODS), and determinations of changes in G_{TE} were done in the Ussing chamber (●). Where indicated by arrows, extracellular calcium was increased to the designated level by adding aliquots from concentrated $CaCl_2$ solution incrementally. The experiment was repeated two times (total of 5 filters) with similar effects. In all cases, Ca_i increased significantly ($P < 0.01$ paired *t*-test); means of Ca_i were 89 ± 6 nM at Ca_o of 1.2 mM and 97 ± 5 nM at Ca_o of 4.0 mM. *B*: effects of increasing osmolarity in the subluminal solution on G_{TE}. Shown is an experiment done on CaSki cells plated on filters and maintained in regular culture medium. Where indicated by arrows, osmolarity in the subluminal solution was increased to the designated level by adding aliquots from concentrated sucrose solution to the subluminal solution incrementally. The experiment was repeated three times (total of 8 filters) with similar effects. In all cases, G_{TE} increased significantly ($P < 0.01$ paired *t*-test); means of G_{TE} were 71 ± 8 mS/cm^2 at isotonic conditions and 105 ± 9 mS/cm^2 at 330 mosmol/l.

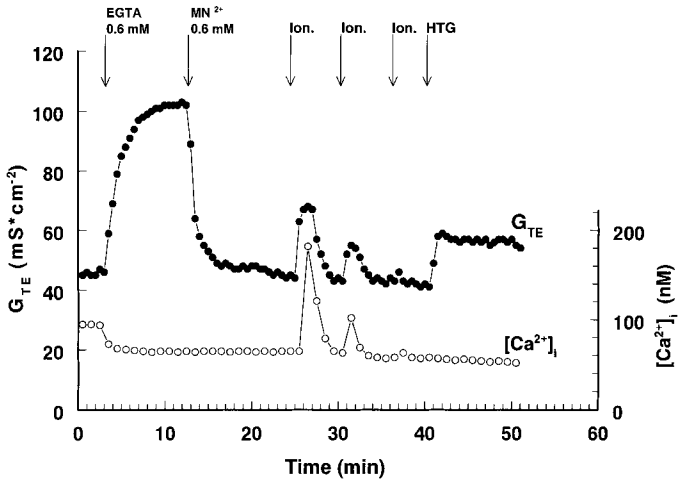

Fig. 2. Experimental design to study effects of lowering extracellular calcium on G_{TE} and on cytosolic calcium. Shown is an experiment done on CaSki cells plated on filters and maintained in regular culture medium. Determinations of changes in G_{TE} were done in the Ussing chamber (●), and determinations of changes in cytosolic calcium were done in the fluorescence chamber (○, see METHODS); data for the two assays are superimposed by time scale. After stabilization, 0.6 mM EGTA was added to lower extracellular calcium from 1.2 to 0.6 mM. After additional 10–15 min, 0.6 mM $MnCl_2$ was added to lower G_{TE} to baseline. Ionomycin (Ion) was added at 5 μM. When indicated, aliquots of 2 M sucrose solution were added to the subluminal compartment to establish a hypertonic gradient (HTG) in the subluminal to luminal direction, where indicated. Experiments were repeated two times, with a total of 5 filters. $[Ca^{2+}]_i$, intracellular calcium concentration.

Mn^{2+} had no effect on intracellular fura 2 fluorescence (Fig. 2).

To determine conditions in which lowering cytosolic calcium does affect permeability, cells were depleted of cytosolic calcium by using repeated administrations of the calcium ionophore ionomycin. In CaSki cells, ionomycin increases cytosolic calcium and G_{TE} transiently and acutely (23). The effect is the result of calcium mobilization from intracellular stores (including mitochondria), and cells replenish intracellular calcium by augmented capacitative calcium influx (23, 28). The duration of the increases in cytosolic calcium and in G_{TE} depends on extracellular calcium: at ≥1.2 mM calcium, the increases last >10 min (23, 28), even if cells are treated with increasing concentrations of ionomycin (Table 1). In cells bathed in low calcium (0.6 mM), the effects are shorter and last only 3–5 min (Fig. 2), probably due to incomplete replenishment of calcium stores (23, 25). Repeat applications of ionomycin to cells bathed in low calcium resulted in smaller increases in cytosolic calcium and in G_{TE}; after a third treatment with ionomycin, there were no additional increases in cytosolic calcium or in G_{TE} (Fig. 2 and Table 1), suggesting that intracellular stores became depleted of calcium. Under these conditions, G_{TE} decreased slowly but persistently (Fig. 2; see also Fig. 3).

The effects of EGTA, Mn^{2+}, ionomycin, and $CaCl_2$ were reversible upon restoring extracellular calcium to 1.2 mM; levels of G_{TE} returned to baseline, and cells regained their responsiveness to ionomycin (data not

Table 1. *Effects of extracellular calcium on ionomycin-induced increases in cytosolic calcium and G_{TE}*

	Extracellular Calcium, mM		
	0.6	1.2	4.0
Estrogen-deficient cells			
Cytosolic calcium			
ΔIncrease above baseline, nM	0	35 ± 5	33 ± 6
Length of increase, min	0	>10	>10
G_{TE}			
ΔIncrease above baseline, mS/cm^2	0	36 ± 9	57 ± 21
Length of increase, min	0	>10	>10
Estrogen-treated cells			
Cytosolic calcium			
ΔIncrease above baseline, nM	0	45 ± 17	41 ± 5
Length of increase, min	0	>10	>10
G_{TE}			
ΔIncrease above baseline, mS/cm^2	0	122 ± 25*	147 ± 11*
Length of increase, min	0	>10	>10

Values are means ± SD of changes in cytosolic calcium and transepithelial electrical conductance (G_{TE}) in response to the third successive addition of ionomycin. Experiments are described in Figs. 2 and 3. *$P < 0.01$ compared with estrogen-deficient cells.

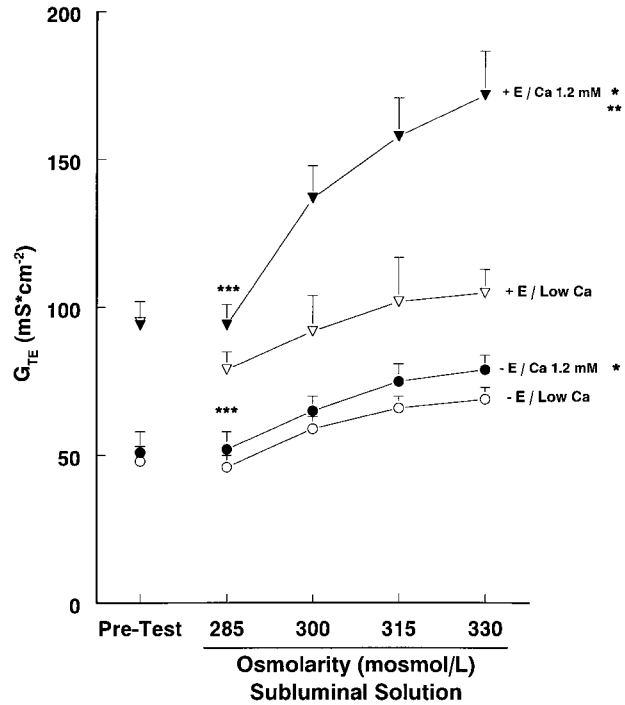

Fig. 3. Effects of estrogen, low extracellular calcium, and hypertonicity on G_{TE} levels. Changes in G_{TE} (means ± SD) were determined in estrogen-deficient (−E) or in estrogen-treated CaSki cells (+E) at the following three time points: *1*) at baseline, before lowering extracellular calcium (Pretest); *2*) 20 min after treatment with 0.6 mM EGTA, 0.6 mM Mn^{2+}, and 5 μM ionomycin (Low Ca, see Fig. 1 for details); these measurements were done in isotonic buffer (285 mosmol/l); *3*) 3 min after increasing the osmolarity of the subluminal solution from 285 mosmol/l to either 300, 315, or 330 mosmol/l. Experiments were repeated three times with 3–6 filters in each experiment. Ca 1.2 mM, experiments done on cells bathed in normal extracellular calcium (1.2 mM). The findings are described in RESULTS. *$P < 0.05$–0.01 (ANOVA) for +E/Ca 1.2 vs. +E/Low Ca and for −E/Ca 1.2 vs. −E/Low Ca. **$P < 0.01$ (ANOVA) for +E/Ca 1.2 vs. −E/Ca 1.2. ***$P < 0.05$ (paired *t*-test) for Ca 1.2 vs. Low Ca in both +E and −E groups.

shown). Staining with MTT was negative, indicating that none of the agents produced toxic effects on the cells. In subsequent experiments, we used treatments with EGTA-Mn^{2+}-ionomycin as the method to lower cytosolic calcium and deplete intracellular calcium stores.

Increases in extracellular calcium to 4.0 mM had no effect on the responses to ionomycin (Table 1).

Estrogen increases baseline permeability and augments effects of hypertonicity and ionomycin. To determine the degree to which changes in cytosolic calcium affect the estrogen-induced increase in paracellular permeability, CaSki cells on filters were treated with 17β-estradiol at the physiological concentration of 10 nM. The following two control conditions were used: *1*) cells grown in estrogen-deficient medium and considered to be estrogen depleted and *2*) cells exposed to a hypertonic gradient in the subluminal to luminal direction. Both treatments with estrogen and hypertonic gradients in the subluminal to luminal direction increase permeability across cultured human cervical epithelia by decreasing the resistance of the lateral intercellular space R_{LIS} (16, 20). However, the effects have different time courses and involve different cellular/molecular mechanisms: treatment with estrogen requires hours (16), whereas hypertonic gradients increase G_{TE} instantaneously (Fig. 1*B* and Refs. 15 and 20). Also, estrogen increases G_{TE} by fragmenting the cytoskeleton (16), whereas hypertonic gradients in the subluminal to luminal direction dilate the lateral intercellular space by stimulating water efflux (15, 20).

Baseline levels of G_{TE} across cultures of estrogen-deprived CaSki cells ranged 51 ± 5 mS/cm^2 (~20 Ω·cm^2; Fig. 3). Treatment with 17β-estradiol increased G_{TE} to 95 ± 5 mS/cm^2 (Fig. 3, $P < 0.01$), confirming our previous studies (16, 24). In estrogen-deficient cells, hypertonic gradients in the subluminal to luminal direction increased G_{TE} acutely (Fig. 2) and in a concentration-related manner (Fig. 3), confirming our previous studies (15, 40). A similar effect was also observed in estrogen-treated cells, but the responses were significantly greater in the latter (Fig. 3). For instance, in estrogen-treated cells, a hypertonic gradient of 45 mosmol/l increased G_{TE} by 83 mS/cm^2 compared with 27 mS/cm^2 in estrogen-deficient cells (Fig. 3, $P < 0.01$). These results indicate that treatment with estrogen increases baseline permeability and that it augments the increase in permeability in response to hypertonic gradients.

Treatment with 17β-estradiol had no significant effect on the ionomycin-induced increase in cytosolic calcium, but it augmented the increase in G_{TE} in response to ionomycin (Table 1). In contrast to hypertonic gradients, changes in G_{TE} in response to ionomycin were critically dependent on extracellular calcium (Fig. 2 and Table 1). We therefore used hypertonic gradients as the second independent method (in addition to estrogen) to determine effects of cytosolic calcium on G_{TE}.

Calcium depletion decreases G_{TE}. The ionomycin-induced depletion of cytosolic calcium decreased G_{TE}. The effect was small in estrogen-deficient cells (Fig. 3), but in estrogen-treated cells G_{TE} decreased significantly by ~20 mS/cm^2 30–40 min after adding EGTA-Mn^{2+}-ionomycin (Fig. 3, 285 mosmol/l). These results indicate that depletion of intracellular calcium decreases permeability to a greater degree in estrogen-treated cells than in estrogen-deficient cells.

Restitution of extracellular calcium to 1.2 mM resulted in a slow but complete reversal of baseline cytosolic calcium and G_{TE} to levels that were observed before the treatments with EGTA-Mn^{2+}-ionomycin (data not shown). Increasing extracellular calcium above 1.2 mM had no effect on baseline G_{TE} (data not shown).

Lowering cytosolic calcium alters the responses to hypertonicity. In estrogen-deficient cells, treatment with EGTA-Mn^{2+}-ionomycin slightly attenuated the responses to hypertonic gradients (Fig. 3). In estrogen-treated cells, treatment with EGTA-Mn^{2+}-ionomycin abrogated the responses to hypertonic gradients; for instance, in estrogen-treated, calcium-depleted cells, a hypertonic gradient of 45 mosmol/l increased G_{TE} only by 25 mS/cm^2 compared with 85 mS/cm^2 in cells bathed in normal calcium (Fig. 3, $P < 0.01$). This result indicates that in estrogen-treated cells most of the increase in permeability in response to hypertonic gradient depends on calcium.

Increasing extracellular calcium above 1.2 mM had no significant effect on the responses to hypertonic gradients, neither in estrogen-deficient nor in estrogen-treated cells (data not shown).

Estrogen modulates cytosolic calcium. To better understand the effect of cytosolic calcium on the responses to hypertonicity, levels of cytosolic calcium were determined in the range of extracellular calcium of 0.6–4.0 mM, and levels of cytosolic calcium were correlated with levels of G_{TE} in response to a hypertonic gradient of 45 mosmol/l in the subluminal to luminal direction. In estrogen-deprived cells, steady-state levels of cytosolic calcium were higher than in estrogen-treated cells (Figs. 4 and 5*A*). Changing extracellular calcium in the range of 0.6–4.0 mM increased cytosolic calcium both in estrogen-deprived cells and in estrogen-treated cells (Figs. 4 and 5*A*), but cytosolic calcium increased more in estrogen-deprived cells than in estrogen-treated cells (Fig. 5*A*).

Changing extracellular calcium also produced concentration-related changes in the hypertonicity-induced increase in permeability (Fig. 4). To determine the degree to which these changes are related to cytosolic calcium, the data in Fig. 4 were analyzed in terms of the net increase in G_{TE} (ΔG_{TE}) relative to changes in cytosolic calcium. In estrogen-treated cells, increases in cytosolic calcium had a greater effect on ΔG_{TE} than in estrogen-deprived cells (Fig. 5*B*). By extrapolation, in estrogen-treated cells cytosolic calcium increased ΔG_{TE} at a rate of 3.0 mS·cm^{-2}·nM cytosolic calcium^{-1} in contrast to 0.3 mS·cm^{-2}·nM cytosolic calcium^{-1} in estrogen-deficient cells (Fig. 5*B*, $P < 0.01$). These results indicate that treatment with estrogen sensitizes cells to cytosolic calcium and promotes larger increase in permeability in response to hypertonicity.

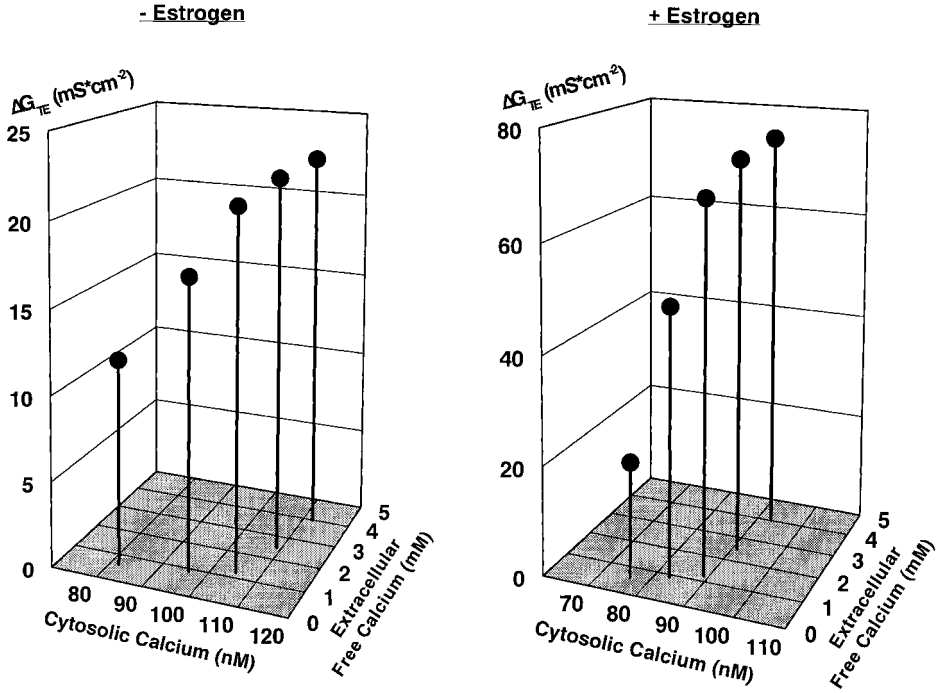

Fig. 4. Effects of changes in extracellular calcium on levels of cytosolic calcium and on changes in G_{TE} in response to subluminal to luminal hypertonic gradient of 45 mosmol/l (ΔG_{TE}). Experiments were done in the Ussing chamber (for measurements of changes in G_{TE}) and in the fluorescent chamber (for measurements of changes in cytosolic calcium) using a design similar to that in Figs. 2 and 3. Levels of extracellular calcium were lowered from 1.2 mM to 0.9 or 0.6 mM by adding 0.3 or 0.6 mM EGTA, respectively, followed by 0.3 or 0.6 mM $MnCl_2$ to restore G_{TE} to baseline levels and 5 μM ionomycin three times to deplete cytosolic calcium. Extracellular calcium was increased to 2.5 and 4.0 mM by adding aliquots from 1 M $CaCl_2$ solution. After treatment (20 min) with EGTA-Mn^{2+}-ionomycin or with $CaCl_2$, aliquots of 2 M sucrose solution were added to the subluminal compartment to establish a hypertonic gradient of 45 mosmol/l in the subluminal to luminal direction. Determinations of cytosolic calcium and changes in G_{TE} were done 3 min after establishing the hypertonic gradient. ΔG_{TE} levels were calculated by subtracting G_{TE} levels that prevailed 10 min after the third addition of ionomycin (see Fig. 2) from G_{TE} levels recorded 3 min after establishing the hypertonic gradient. Shown are mean levels of cytosolic calcium (x-axis) and ΔG_{TE} (z-axis); experiments were repeated three times, with 3–5 filters in each experiment. Variability ranged 7–11% (also see Fig. 5).

Cytosolic calcium does not modulate the effects of sodium nitroprusside and bromo-cGMP on G_{TE}. A possible explanation for the results shown in Figs. 4 and 5 is that calcium regulates critical steps along the signaling cascade that mediates the estrogen increase in permeability. Estrogen increases transcervical paracellular permeability by a mechanism that involves estrogen receptor α-activation of the NO/cGMP-depen-

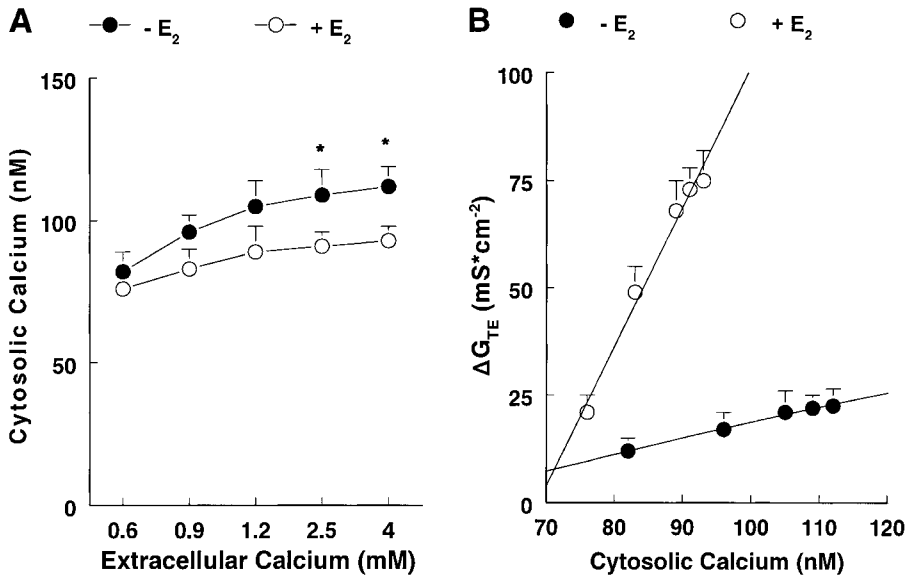

Fig. 5. *A*: mean ± SD of levels of cytosolic calcium as a function of changes in extracellular calcium in estrogen-deprived cells ($-E_2$, ●) and in estrogen-treated cells ($+E_2$, ○). There were three experiments with 3–6 filters in each experiment. Data were derived from Fig. 4. *$P < 0.05$. *B*: mean ± SD of changes in G_{TE} (ΔG_{TE}) in response to subluminal to luminal hypertonic gradient of 45 mosmol/l in estrogen-deprived cells ($-E_2$, ●) and in estrogen-treated cells ($+E_2$, ○) as a function of levels of cytosolic calcium. There were three experiments with 3–6 filters in each experiment. Data of ΔG_{TE} concentration vs. cytosolic calcium concentration were derived from Fig. 4 and were fitted in straight lines ($P < 0.01$ in both cases). The curve in estrogen-treated cells was significantly steeper than in estrogen-deprived cells ($P < 0.01$, ANOVA).

dent increase in G-actin (18, 24). The objectives of the following two experiments were to test the degree to which the effects of NO and cGMP on G_{TE} are dependent on calcium.

The first experiment tested effects of calcium on the responses to sodium nitroprusside (SNP) and 8-bromo (Br)-cGMP. SNP, an NO donor, and 8-Br-cGMP, a stable cell-permeable analog of cGMP, can also increase G_{TE} by upregulation of G-actin (17, 24). In estrogen-deprived cells bathed in normal calcium, SNP or 8-Br-cGMP increased G_{TE} by ~50 mS/cm^2 above baseline (Fig. 6*A*, compare with Fig. 3). A similar effect was observed in cells treated with EGTA-Mn^{2+}-ionomycin (Fig. 6*A*), indicating that lowering cytosolic calcium does not modulate effects of SNP or of 8-Br-cGMP on permeability. In SNP- or in 8-Br-cGMP-treated cells, hypertonicity increased G_{TE} further by ~75 mS/cm^2, regardless whether the cells were previously treated with EGTA-Mn^{2+}-ionomycin (Fig. 6*A*). This is in contrast to the effect in estrogen-treated cells where treatment with EGTA-Mn^{2+}-ionomycin attenuated the increase in G_{TE} in response to hypertonicity (Figs. 3 and 6*A*).

The second experiment tested the effects of calcium on the SNP-, 8-Br-cGMP-, and estrogen-induced increase in G-actin (Fig. 6*B*). The experimental design was similar to that in Fig. 6*A*, except that the end point was G-actin. In estrogen-deprived cells, SNP and Br-cGMP increased G-actin sixfold compared with control cells, regardless if cells were bathed in normal calcium (Fig. 6*B*) or if they were treated with EGTA-Mn^{2+}-ionomycin (Fig. 6*B*). This result differed from that in cells treated with estrogen: in estrogen-treated cells that were incubated in normal calcium, G-actin was 2.5-fold higher than in estrogen-deficient cells; when calcium was lowered with EGTA-Mn^{2+}-ionomycin, G-actin was only 1.2-fold higher (Fig. 6*B*, $P < 0.02$). Collectively, the results shown in Fig. 5, *A* and *B*, indicate that lowering calcium attenuates the hypertonicity-dependent increase in G_{TE} and the increase in G-actin induced by estrogen, but not by SNP or by 8-Br-cGMP.

Calcium modulates the estrogen increase in NO synthesis. A possible explanation for the lack of effect of lowering calcium on the SNP- or 8-Br-cGMP-induced increase in G-actin and in the hypertonicity-induced increase in G_{TE} is that calcium regulates signaling steps more proximal to the action of NO. The three experiments in this section tested the hypothesis that the calcium-sensitive step is estrogen upregulation of NO.

NO is synthesized from L-arginine during the NOS-catalyzed conversion of L-arginine to L-citrulline (1, 36, 39). The first experiment tested the effects of estrogen and calcium on NO release. CaSki cells release NO constitutively in the extracellular medium (Fig. 7*A* and Ref. 17). In estrogen-deficient cells, L-NAME, an NOS inhibitor (10), decreased NO release slightly; in estrogen-treated cells, L-NAME decreased NO release markedly to levels that were observed in estrogen-deficient cells. This result indicates that most of the

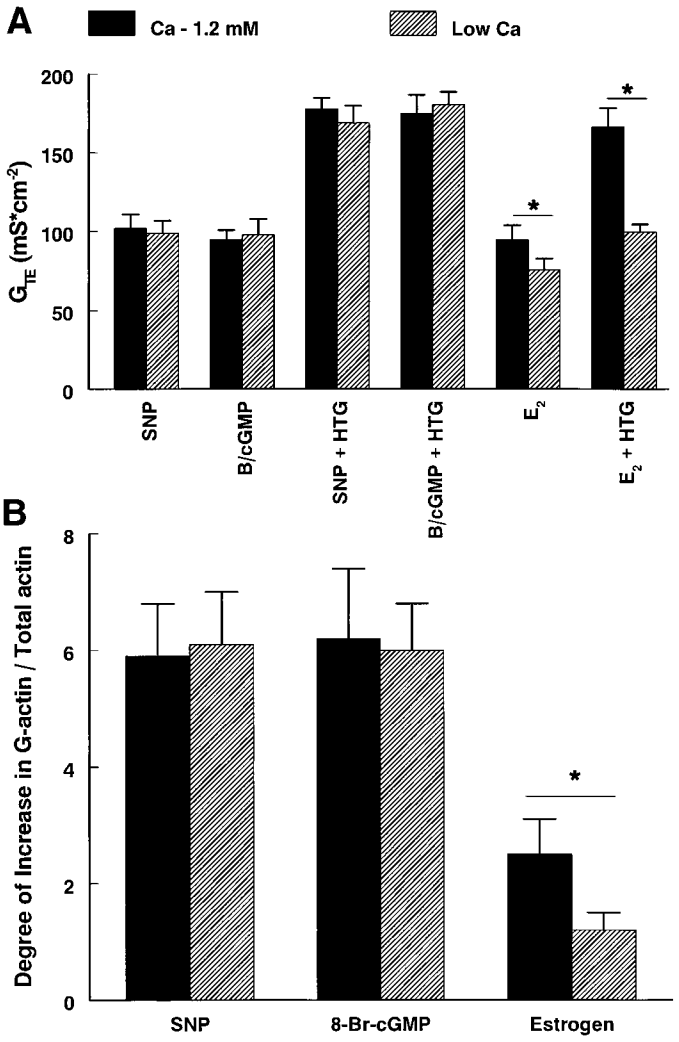

Fig. 6. Effects of treatments with sodium nitroprusside (SNP; 1 mM), 8-bromo (Br)-cGMP (50 μM, B/cGMP), and 17β-estradiol (10 nM, E_2) and of lowered extracellular calcium on changes in G_{TE} in response to subluminal to luminal hypertonic gradient of 45 mosmol/l (*A*) and on levels of G-actin (*B*). Cells were grown on filters in steroid-free medium and were treated with one of the specified agents. When indicated, SNP or 8-Br-cGMP was added 30 min before assays. Filled bars, experiments done on cells bathed in normal calcium (1.2 mM); hatched bars, cells treated with EGTA-Mn^{2+}-ionomycin as described in Figs. 2 and 3. Bars are means ± SD of 4 experiments with 3–5 filters. *$P < 0.05$–0.01.

increase in NO release in estrogen-treated cells originates from NOS(s).

In estrogen-deficient cells, treatment with EGTA-Mn^{2+}-ionomycin decreased NO release from 16 to 12 pmol·min^{-1}·mg protein^{-1} (Fig. 7*A*, $P < 0.01$, paired *t*-test). In estrogen-treated cells, NO release was fourfold greater than in estrogen-deficient cells (Fig. 7*A*), and treatment with EGTA-Mn^{2+}-ionomycin decreased NO release to levels that were observed in estrogen-deprived cells (Fig. 7*A*). This result indicates that most of the estrogen-induced increase in NO release is calcium dependent.

The second experiment tested the calcium requirements of NOS(s) in vitro, in broken cell preparations,

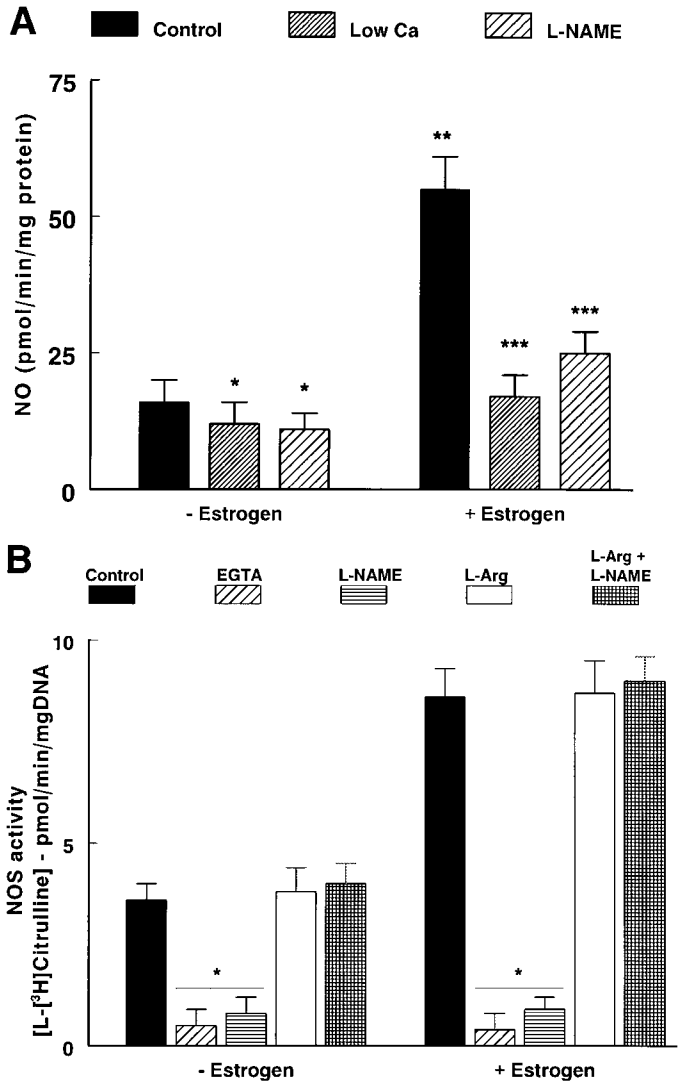

Fig. 7. *A*: modulation of nitric oxide (NO) release from intact CaSki cells. Cells were grown on filters in steroid-free medium in the absence (−Estrogen) or presence (+Estrogen) of 10 nM 17β-estradiol. NO release was measured in dishes containing cells incubated in 1.2 mM calcium before (control, filled bars) and after treatments with EGTA-Mn^{2+}-ionomycin (as in Figs. 2 and 3; Low Ca) or after adding 1 mM N^G-nitro-L-arginine methyl ester (L-NAME; see METHODS). $^*P < 0.01$ compared with control/−Estrogen (paired *t*-test). $^{**}P < 0.01$ compared with control/−Estrogen. $^{***}P < 0.01$ compared with control/+Estrogen (paired *t*-test). Bars are means ± SD of 2 experiments with 3–6 filters in each experiment. *B*: modulation of nitric oxide synthase (NOS) activity in lysates of CaSki cells. Cells were grown on filters in steroid-free medium in the absence (−Estrogen) or presence (+Estrogen) of estrogen. Cells were lysed, and reactions were carried out in the absence (control) or presence of one or more of the following agents: 1.2 mM EGTA, 1 mM L-NAME, or 1 mM L-arginine (L-Arg). $^*P < 0.01$ compared with control in each group (paired *t*-test). Bars are means ± SD of 3 experiments with 3–5 filters in each experiment.

by measuring the effect of calcium on the conversion of L-[2,3,4,5-^{3}H]arginine to L-[2,3,4,5-^{3}H]citrulline. NOS activity in lysates of estrogen-treated cells was 8.6 ± 0.7 pmol·min^{-1}·mg DNA^{-1} and was significantly higher than in estrogen-deficient cells (3.5 ± 0.4 pmol·min^{-1}·mg DNA^{-1}). Addition of EGTA to chelate calcium to <0.1 mM decreased NOS activity to ~0.5 pmol·min^{-1}·mg DNA^{-1}, both in lysates of estrogen-treated cells and in lysates of estrogen-deficient cells (Fig. 7*B*). L-NAME had a similar effect to that of EGTA (Fig. 7*B*). L-Arginine, a naturally occurring substrate for NOS, had no significant effect on NOS activity; however, coadministration of L-arginine with L-NAME blocked the inhibitory effect of L-NAME (Fig. 7*B*). These results indicate that most of the estrogen-induced increase in NO release originates from calcium-dependent, in vitro NOS(s)-dependent conversion of L-citrulline to L-arginine.

Three different broad categories of NOS isoforms have been characterized and classified according to the calcium dependency of the enzyme: the endothelial [eNOS (NOS-3)] and neuronal [bNOS (NOS-1)] isozymes exhibit strict dependency on intracellular calcium/calmodulin levels, whereas the inducible NOS [iNOS (NOS-2)] is less dependent on calcium (1, 36, 39). Human cervical epithelial cells express mRNA for all three isoforms (17), and estrogen has been shown to upregulate the eNOS (23). In contrast, relatively little is known about the calcium dependence of the eNOS in human cervical cells. The third experiment tested the effects of calcium and estrogen on the expression of eNOS, bNOS, and iNOS mRNA using the RT-PCR technique. The present study confirmed our previous results that CaSki cells express mRNA for the eNOS, bNOS, and iNOS and that treatment with estrogen upregulated steady-state levels of eNOS mRNA (Fig. 7 and Ref. 17). Treatment with 17β-estradiol had no significant effect on the expression of mRNA for GAPDH, bNOS, or iNOS. In contrast, estrogen upregulated eNOS mRNA; densitometry analysis of three experiments revealed that estradiol increased the ratio of eNOS to GAPDH mRNA 9-, 17-, and 25-fold (Fig. 8).

In estrogen-deficient cells, treatment with EGTA-Mn^{2+}-ionomycin had no significant effect on the expression of mRNA of GAPDH, eNOS, bNOS, or iNOS (Fig. 8); densitometry analysis of three experiments revealed that the ratio of eNOS to GAPDH mRNA in cells treated with EGTA-Mn^{2+}-ionomycin was 0.5, 1.0, and 1.3 compared with control cells. In estrogen-treated cells, additional treatment with EGTA-Mn^{2+}-ionomycin did not modulate the estrogen increase in eNOS mRNA (Fig. 8). These results indicate that estrogen upregulates eNOS and that lowering cytosolic calcium does not modulate the effect of estrogen.

DISCUSSION

The results of the present study provide novel data about the regulation of transcervical permeability by estrogen and by cytosolic calcium. Treatment with estrogen augmented increases in permeability that were induced by ionomycin and hypertonicity. Although all three agents/conditions increase permeability by decreasing the resistance of the lateral intercellular space, R_{LIS} (15, 20, 28), the cellular mechanisms of action are different: estrogen increases permeability by fragmenting the cytoskeleton (present results and Ref.

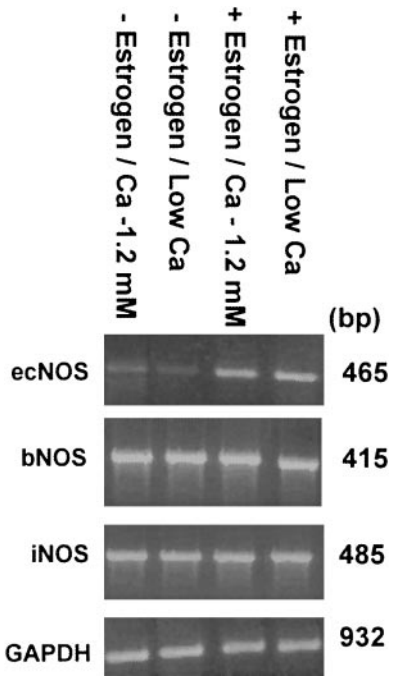

Fig. 8. Effects of estrogen and calcium on the expression of mRNA for endothelial NOS (eNOS), brain NOS (bNOS), and inducible NOS (iNOS) in CaSki cells. The experiments utilized the RT-PCR technique and were done on lysates of cells cultured on filters in steroid-free medium in the absence (−Estrogen) or presence (+Estrogen) of 10 nM 17β-estradiol. Also tested were the effects of lowering extracellular calcium from 1.2 to 0.6 mM by treatments with EGTA, Mn^{2+}, and ionomycin, as in Figs. 2 and 3. Oligonucleotide primers complementary to the cloned eNOS, bNOS, and iNOS were used to amplify single cDNA fragments of 465, 415, and 485 bp, respectively. In mock reactions [lacking the oligo(dT) and the avian myeloblastosis virus; see METHODS], no detectable bands were found (data not shown). The experiment was repeated 3 times with similar trends. GAPDH, glyceraldehyde-3-phosphate dehydrogenase.

16); ionomycin and hypertonicity generate a subluminal to luminal hydrostatic gradients. Ionomycin stimulates Cl^- secretion, followed by water efflux (15, 20); hypertonicity stimulates water efflux directly (15). In both cases, water moves from the cells into the intercellular space; water that accumulates in the basal compartment of the intercellular space dilates the space and generates a subluminal to luminal hydrostatic gradient (32, 45). The effects of estrogen on G-actin and on the cytoskeleton can explain how estrogen augments the responses to ionomycin and hypertonicity; changes in cell size depend on the flexibility of the cytoskeleton, and cells with a fragmented cytoskeleton can adapt more readily to changes in cell volume (6, 7, 9, 44).

Estrogen, ionomycin, and hypertonicity activate a common paracellular mechanism, namely, a decrease in R_{LIS} (15, 20, 28). This finding has physiological relevance because in vivo the main driving force for fluid transudation across the cervical epithelium is the pressure generated by the blood in the subepithelial space (14), which is equivalent to a hydrostatic gradient in the subluminal to luminal direction.

The experiments of the present study also showed that baseline permeability and the responses to hypertonicity depend on cytosolic calcium. The results showed that *1*) increases in cytosolic calcium had little effect on baseline permeability; in contrast, lowering cytosolic calcium decreased baseline permeability, suggesting that physiological resting steady-state cytosolic calcium levels induce a maximal degree of permeability. *2*) Lowering cytosolic calcium attenuated the increase in permeability in response to hypertonicity, whereas increasing cytosolic calcium augmented the response. The critical factor relative to the status of cytosolic calcium was resting levels of cytosolic calcium, as determined by cellular calcium content, rather than the cell's ability to increase cytosolic calcium by mobilization from intracellular stores, since treatment with the endoplasmic reticulum calcium pump inhibitor thapsigargin had no significant effect on permeability (results not shown). *3*) Lowering cytosolic calcium blocked the estrogen-induced increase in G-actin, and it attenuated the augmented increase in permeability in response to hypertonicity, indicating that the estrogen-related, hypertonicity-induced increase in permeability is calcium dependent.

The estrogen increase in G-actin and in the permeability involves four key signaling steps: the α-estrogen receptor, eNOS, NO, and cGMP (16, 17, 18, 24). Agents that mimic effects of NO (e.g., SNP) and cGMP (e.g., 8-Br-cGMP) can increase G-actin and the permeability (present results and Refs. 17, 18, 28). Lowering cytosolic calcium had no effect on the responses to SNP or to 8-Br-cGMP; in contrast, lowering cytosolic calcium abrogated the estrogen-induced increase in NO release from intact cells, and it attenuated the estrogen-induced increase in the conversion of L-citrulline to L-arginine. In addition, estrogen increased expression of mRNA for the calcium-dependent eNOS. Collectively, these results suggest that the calcium-dependent rate-limiting step is NO synthesis by the calcium-dependent eNOS.

In estrogen-deficient cells bathed in low calcium, the responses to hypertonic gradients were mildly attenuated compared with responses in cells bathed in normal calcium, suggesting some involvement of calcium also in the response to hypertonicity. A possible explanation is that lowering calcium blocked the activity of calcium-dependent NOS(s) that produce(s) NO constitutively, even in cells grown in steroid-free conditions. This statement is supported by the findings that CaSki cells (present study) and other types of cultured human cervical epithelial cells express mRNA for all three NOS isoforms and that the cells constitutively secrete NO (present results and Ref. 17). Another source of NO is from calcium-independent NOS; lowering cytosolic calcium abrogated the estrogen-induced increase in the conversion of L-citrulline to L-arginine, and the remaining NO activity could be blocked by L-NAME, indicating that some of the NO activity is contributed by calcium-independent mechanisms, possibly by the iNOS (33). These results support our hypothesis (17) that cervical cells autoregulate permeability and maintain increased paracellular permeability by continuously secreting NO. Accordingly, the effect of NO in-

volves autocrine/paracrine regulation of permeability: cells secrete NO, and NO can either act on the same cell (autocrine regulation) or diffuse into neighboring cells (paracrine regulation). This hypothesis explains the slow decrease in permeability in cultures treated with EGTA-Mn^{2+}-ionomycin; depletion of calcium may have decreased NO synthesis and abrogated its effect on permeability (4). It also explains the greater decrease in permeability in estrogen-treated cells than in estrogen-deficient cells because estrogen increases NO (present results and Refs. 8, 12, 42), and blocking NO synthesis would have a greater impact on permeability.

Previous studies in smooth muscle cells reported that estrogen could directly block calcium channels and attenuate calcium influx, thus lowering cytosolic calcium (5, 35, 37, 48). The present experiments show similar trends in human cervical epithelial cells in that baseline levels of cytosolic calcium were lower in estrogen-treated cervical cells than in estrogen-deficient cells. The mechanism by which estrogen lowers cytosolic calcium in cervical epithelial cells is unclear. Changing extracellular calcium in the range of 0.6–4.0 mM increased cytosolic calcium in a concentration-related manner, both in estrogen-treated cells and in estrogen-deficient cells. Extracellular calcium levels >1.2 mM increased cytosolic calcium more in estrogen-deficient cells than in estrogen-treated cells, raising the possibility that estrogen blocks calcium channels also in cervical cells.

Relatively little is known about the biological role of the lowered cytosolic calcium in estrogen-treated cells. Because both estrogen and calcium upregulate NO (present results), it is possible that the lowered cytosolic calcium controls NO activity and prevents apoptosis (3, 29). However, more studies are needed to clarify this issue.

The results of the present study may be important for understanding regulation of cervical secretions in vivo because agonists that elevate cytosolic calcium can activate the eNOS (36, 39). Secretagogues, neurotransmitters, and agonists that participate in the inflammatory response can stimulate an increase in cytosolic calcium in human cervical cells (23). These agents may stimulate NO production, increase G-actin, and lead to increased paracellular permeability. Increased permeability will allow greater fluxes of fluids and solutes from the blood into the cervical canal and augment secretion of cervical mucus. In cervical cells, estrogen increases NO by upregulation of the calcium-dependent eNOS (present study). Subsequently, changes in cytosolic calcium are likely to affect permeability more in estrogen-treated cells than in estrogen-deprived cells. This conclusion may have pharmacological significance in the sense of modulating cervical secretions directly by NO-related agents, but more studies are needed to clarify the effects in women.

The study was supported by National Institutes of Health Grants HD-00977, HD-29924, and AG-15955.

REFERENCES

1. **Archer S.** Measurement of nitric oxide in biological models. *FASEB J* 7: 349–360, 1993.
2. **Blikstad I, Markey F, Carlsson L, Persson T, and Lindberg U.** Selective assay of monomeric and filamentous actin in cell extracts, using inhibition of deoxyribonuclease 1. *Cell* 5: 935–943, 1978.
3. **Brune B, Gotz C, Messmer UK, Sandau K, Hirvonen MR, and Lapetina EG.** Superoxide formation and macrophage resistance to nitric oxide-mediated apoptosis. *J Biol Chem* 272: 7253–7258, 1997.
4. **Cho MM, Ziats NP, Pal D, Utian WH, and Gorodeski GI.** Estrogen modulates paracellular permeability of human umbilical vein endothelial cells by and iNOS related mechanisms. *Am J Physiol Cell Physiol* 276: C337–C349, 1999.
5. **Collins P, Rosano GM, Jiang C, Lindsay D, Sarrel PM, and Poole-Wilson PA.** Cardiovascular protection by oestrogen—a calcium antagonist effect? *Lancet* 341: 1264–1265, 1993.
6. **De La Cruz EM and Pollard TD.** Kinetics and thermodynamics of phalloidin binding to actin filaments from three divergent species. *Biochemistry* 35: 14054–14061, 1996.
7. **Dufort PA and Lumsden CJ.** How profilin/barbed-end synergy controls actin polymerization: a kinetic model of the ATP hydrolysis circuit. *Cell Motil Cytoskeleton* 35: 309–330, 1996.
8. **Farre J, de Miguel LS, Gonzalez-Fernandez F, Arriero MD, Rico L, Garcia R, Casado S, and Lopez-Farre A.** Estrogen stimulates neuronal nitric oxide synthase protein expression in human neutrophils. *Circ Res* 85: 1020–1026, 1999.
9. **Foskett JK.** The role of calcium in the control of volume regulatory transport pathways. In: *Cellular and Molecular Physiology of Cell Volume Regulation*. Boca Raton, FL: CRC, 1994, p. 259–278.
10. **Garvey EP, Oplinger JA, Tanoury GJ, Sherman PA, Fowler M. Marshall S, Harmon MF, Paith JE, and Furfine ES.** Potent and selective inhibition of human nitric oxide synthases. *J Biol Chem* 269: 26669–26676, 1994.
11. **Geller DA, Lowenstein CJ, Shapiro RA, Nussler AK, Di Silvio M, Wang SC, Nakayama DK, Simmons RL, Snyder SH, and Billiar TR.** Molecular cloning and expression of inducible nitric oxide synthase from human hepatocytes. *Proc Natl Acad Sci USA* 90: 3491–3495, 1993.
12. **Goetz RM, Thatte HS, Prabhakar P, Cho MR, Michel T, and Golan DE.** Estradiol induces the calcium-dependent translocation of endothelial nitric oxide synthase. *Proc Natl Acad Sci USA* 96: 2788–2793, 1999.
13. **Gonzalez-Mariscal L, Contreras RG, Bolivar JJ, Ponce A, Chavez de Ramirez B, and Cereijido M.** Role of calcium in tight junction formation between epithelial cells. *Am J Physiol Cell Physiol* 259: C978–C986, 1990.
14. **Gorodeski GI.** The cervical cycle. In: *Reproductive Endocrinology, Surgery, and Technology*, edited by Adashi EY, Rock JA, and Rosenwaks Z. Philadelphia, PA: Lippincott-Raven, 1996, p. 301–324.
15. **Gorodeski GI.** The cultured human cervical epithelium: a new model for studying transepithelial paracellular transport. *J Soc Gynecol Investig* 3: 267–280, 1996.
16. **Gorodeski GI.** Estrogen increases the permeability of the cultured human cervical epithelium by modulating cell deformability. *Am J Physiol Cell Physiol* 275: C888–C899, 1998.
17. **Gorodeski GI.** NO increases permeability of cultured human cervical epithelia by cGMP-mediated increase in G-actin. *Am J Physiol Cell Physiol* 278: C942–C952, 2000.
18. **Gorodeski GI**. Role of nitric oxide and cGMP in the estrogen regulation of cervical epithelial permeability *Endocrinology* 141: 1658–1666, 2000.
19. **Gorodeski GI, Burfeind F, Uin GS, Pal D, and Abdul-Karim F.** Regulation by retinoids of P2Y2 nucleotide receptor mRNA in human uterine cervical cells. *Am J Physiol Cell Physiol* 275: C758–C765, 1998.
20. **Gorodeski GI, De Santis BJ, Goldfarb J, Utian WH, and Hopfer U.** Osmolar changes regulate the paracellular permeability of cultured human cervical epithelium. *Am J Physiol Cell Physiol* 269: C870–C877, 1995.

21. **Gorodeski GI, Eckert RL, Utian WH, and Rorke EA.** Maintenance of in vivo-like keratin expression, sex steroid responsiveness and estrogen receptor expression in cultured human ectocervical epithelial cells. *Endocrinology* 126: 399–406, 1990.
22. **Gorodeski IG, Geier A, Lunenfeld B, Beery R, and Bahary CM.** Progesterone (P) receptor dynamics in estrogen primed normal human cervix following P injection. *Fertil Steril* 47: 108–113, 1987.
23. **Gorodeski GI, Hopfer U, and Wenwu J.** Purinergic receptor induced changes in paracellular resistance across cultures of human cervical cells are mediated by two distinct cytosolic calcium related mechanisms. *Cell Biochem Biophys* 29: 281–306, 1998.
24. **Gorodeski GI and Pal D.** Involvement of estrogen receptors α and β in the regulation of cervical permeability. *Am J Physiol Cell Physiol* 278: C689–C696, 2000.
25. **Gorodeski GI, Peterson D, De Santis BJ, and Hopfer U.** Nucleotide-receptor mediated decrease of tight-junctional permeability in cultured human cervical epithelium. *Am J Physiol Cell Physiol* 270: C1715–C1725, 1996.
26. **Gorodeski GI, Romero MF, Hopfer U, Rorke E, Utian WH, and Eckert RL.** Human uterine cervical epithelial cells grown on permeable support—a new model for the study of differentiation and transepithelial transport. *Differentiation* 56: 107–118, 1994.
27. **Gorodeski GI, Wenwu J, and Hopfer U.** Extracellular Ca^{2+} directly regulates tight junctional permeability in the human cervical cell line CaSki. *Am J Physiol Cell Physiol* 272: C511–C524, 1997.
28. **Gorodeski GI and Whittembury J.** A novel fluorescence chamber for the determination of volume changes in human CaSki cell cultures attached on filters. *Cell Biochem Biophys* 29: 307–332, 1998.
29. **Gow AJ, Thom SR, and Ischiropoulos H.** Nitric oxide and peroxynitrite-mediated pulmonary cell death. *Am J Physiol Lung Cell Mol Physiol* 274: L112–L118, 1998.
30. **Grynkiewicz G, Poenie M, and Tsien RY.** A new generation of Ca^{2+} indicators with greatly improved fluorescence properties. J Biol Chem 260: 3440–3450, 1985.
31. **Jovov B, Lewis SA, Crowe WE, Berg JR, and Wills NK.** Role of intracellular Ca^{2+} in modulation of tight junction resistance in A6 cells. *Am J Physiol Renal Fluid Electrolyte Physiol* 266: F775–F784, 1994.
32. **Kondo M, Finkbeiner WE, and Widdicombe JH.** Changes in permeability of dog tracheal epithelium in response to hydrostatic pressure. *Am J Physiol Lung Cell Mol Physiol* 262: L176–L182, 1992.
33. **Kone BC and Baylis C.** Biosynthesis and homeostatis roles of nitric oxide in the normal kidney. *Am J Physiol Renal Physiol* 272: F561–F578, 1997.
34. **Lamas S, Marsden PA, Li GK, Tempst P, and Michel T.** Endothelial nitric oxide synthase: molecular cloning and characterization of a distinct constitutive enzyme isoform. *Proc Natl Acad Sci USA* 89: 6348–6352, 1992.
35. **Lippert TH, Seeger H, Mueck AO, Hanke H, and Haasis R.** Effect of estradiol, progesterone and progestogens on calcium influx in cell cultures of human vessels. *Menopause* 3: 33–37, 1996.
36. **Moncada S, Palmer RMJ, and Higgs EA.** Nitric oxide: physiology, pathophysiology and pharmacology. *Pharmacol Rev* 43: 109–142, 1991.
37. **Murphy JG and Khalil RA.** Decreased [Ca(2+)](i) during inhibition of coronary smooth muscle contraction by 17beta-estradiol, progesterone, and testosterone. *J Pharmacol Exp Ther* 291: 44–52, 1999.
38. **Nakane M, Schmidt HHHW, Pollock JS, Forstermann U, and Murad F.** Cloned human brain nitric oxide synthase is highly expressed in skeletal muscle. *FEBS Lett* 316: 175–180, 1993.
39. **Nathan C**. Nitric oxide as a secretory product of mammalian cells. *FASEB J* 6: 3051–3064, 1992.
40. **Persson BE and Spring KR.** Gallbladder epithelial cell hydraulic water permeability and volume regulation. *J Gen Physiol* 79: 481–505, 1982.
41. **Reuss L.** Tight junction permeability to ions and water. In: *Tight-Junctions*, edited by Cereijido M. Boca Raton, FL: CRC, 1991, p. 49–66.
42. **Saito S, Aras RS, Lou H, Ramwell PW, and Foegh ML.** Effects of estrogen on nitric oxide synthase expression in rat aorta allograft and smooth muscle cells. *J Heart Lung Transplant* 18: 937–945, 1999.
43. **Salter M, Knowles RG, and Moncada S.** Widespread tissue distribution, species distribution and changes in activity of Ca^{2+}-dependent and Ca^{2+}-independent nitric oxide synthases. *FEBS Lett* 291: 145–149, 1991.
44. **Sheterline P, Clayton J, and Sparrow J.** Actin. *Protein Profile* 2: 1–103, 1995.
45. **Spring KR and Hope A.** Size and shape of the lateral intercellular spaces in a living epithelium. *Science* 200: 54–58, 1978.
46. **Stangel M, Zettl UK, Mix E, Zielasek J, Toyka KV, Hartung HP, and Gold R.** H_2O_2 and nitric oxide-mediated oxidative stress induce apoptosis in rat skeletal muscle myoblasts. *J Neuropathol Exp Neurol* 55: 36–43, 1996.
47. **Ussing HH and Zerahn K.** Active transport of sodium as the source of electric current in the short-circuited isolated frog skin. *Acta Physiol Scand* 23: 110–127, 1951.
48. **Yamamoto T.** Effects of estrogens on Ca channels in myometrial cells isolated from pregnant rats. *Am J Physiol Cell Physiol* 268: C64–C69, 1995.